Virologica Sinica (2021) 36:958–967
https://doi.org/10.1007/s12250-021-00359-x

www.virosin.org
www.springer.com/12250

RESEARCH ARTICLE

Establishment of a Reverse Genetic System of Severe Fever with Thrombocytopenia Syndrome Virus Based on a C4 Strain

Mingyue Xu[1,2] · Bo Wang[1] · Fei Deng[1] · Hualin Wang[1] · Manli Wang[1] · Zhihong Hu[1] · Jia Liu[1]

Received: 18 December 2020 / Accepted: 21 January 2021 / Published online: 15 March 2021

Abstract

Severe fever with thrombocytopenia syndrome virus (SFTSV) is an emerging tick-borne bunyavirus that causes hemorrhagic fever-like disease (SFTS) in humans with a case fatality rate up to 30%. To date, the molecular biology involved in SFTSV infection remains obscure. There are seven major genotypes of SFTSV (C1–C4 and J1–J3) and previously a reverse genetic system was established on a C3 strain of SFTSV. Here, we reported successfully establishment of a reverse genetics system based on a SFTSV C4 strain. First, we obtained the 5′- and 3′-terminal untranslated region (UTR) sequences of the Large (L), Medium (M) and Small (S) segments of a laboratory-adapted SFTSV C4 strain through rapid amplification of cDNA ends analysis, and developed functional T7 polymerase-based L-, M- and S-segment minigenome assays. Then, full-length cDNA clones were constructed and infectious SFTSV were recovered from co-transfected cells. Viral infectivity, growth kinetics, and viral protein expression profile of the rescued virus were compared with the laboratory-adapted virus. Focus formation assay showed that the size and morphology of the foci formed by the rescued SFTSV were indistinguishable with the laboratory-adapted virus. However, one-step growth curve and nucleoprotein expression analyses revealed the rescued virus replicated less efficiently than the laboratory-adapted virus. Sequence analysis indicated that the difference may be due to the mutations in the laboratory-adapted strain which are more prone to cell culture. The results help us to understand the molecular biology of SFTSV, and provide a useful tool for developing vaccines and antivirals against SFTS.

Keywords Bunyavirus · Severe fever with thrombocytopenia syndrome virus (SFTSV) · Minigenome · Reverse genetic system · T7 polymerase · C4 strain

Introduction

Severe fever with thrombocytopenia syndrome (SFTS) is an emerging hemorrhagic fever disease, which was first reported in 2009 in China (Yu *et al.* 2011). The disease was subsequently reported in South Korea, Japan, the United States, and Vietnam (McMullan *et al.* 2012; Park *et al.* 2016; Takahashi *et al.* 2014; Tran *et al.* 2019). The major clinical symptoms of SFTS include severe fever, thrombocytopenia, and leukopenia. SFTS is also frequently associated with gastrointestinal symptoms, and even multiple-organ failure in most dying patients, with a high case fatality rate up to 30% (McMullan *et al.* 2012; Zhao *et al.* 2012). The cause pathogen is a newly identified tick-borne virus (SFTSV) (Yu *et al.* 2011), and the disease is usually associated with tick bites but can also be transmitted from human to human occasionally (Liu *et al.* 2012; Wang *et al.* 2014). Considering increasing number of

Electronic supplementary material The online version of this article (https://doi.org/10.1007/s12250-021-00359-x) contains supplementary material, which is available to authorized users.

✉ Jia Liu
liujia@wh.iov.cn

✉ Zhihong Hu
huzh@wh.iov.cn

✉ Manli Wang
wangml@wh.iov.cn

[1] State Key Laboratory of Virology and National Virus Resource Center, Wuhan Institute of Virology, Center for Biosafety Mega-Science, Chinese Academy of Sciences, Wuhan 430071, China

[2] University of the Chinese Academy of Sciences, Beijing 100049, China

reported cases since its first outbreak, and lacking of effective vaccines or antiviral drugs, SFTS poses a global threat to public health, necessitating further investigation of the molecular biology and pathogenesis mechanisms involved in SFTSV infection (Cyranoski 2018).

SFTSV is a member of the *Bandavirus* genus belonging to the *Phenuiviridae* family in the order of *Bunyavirales* (Liu *et al.* 2019; Maes *et al.* 2019). It is an enveloped RNA virus with tripartite, single-stranded, negative-sense or ambisense RNA genomes: the Large (L) segments encodes a RNA-dependent RNA polymerase (RdRp); the Medium (M) segment encodes a surface glycoprotein precursor, which is further processed into Gn and Gc; and the Small (S) segment encodes the nucleoprotein (NP) and a non-structural protein (NSs) with an ambisense coding strategy (Guardado-Calvo and Rey 2017; Yu *et al.* 2011). In bunyaviruses, the NP and RdRp associate with viral genome RNA to form active ribonucleoprotein complexes (RNPs), which are necessary for viral genome replication, resulting in complementary RNA (cRNA) (positive sense) and progeny genomic vRNA (negative sense) (Walter and Barr 2011). The untranslated regions (UTRs) at both the 5′ and 3′ ends of each genome segment serve as a promoter and terminator, and are required for replication, transcription, and packaging of the viral genome. These UTRs containing signals direct the RdRp to perform transcription and replication (Brennan *et al.* 2015; Elliott 2014).

Reverse genetics systems are powerful tools for exploring molecular biology and pathogenesis of RNA viruses and also for vaccine and antiviral drugs development, due to the ability to generate recombinant viruses from cloned cDNA. It is demonstrated that virus transcription, replication, and genome packaging require the cis-acting elements in the 5′ and 3′ UTRs of RNA genomes and the trans-acting viral RdRp and NP (Barr and Wertz 2005; Bergeron *et al.* 2010; Flick *et al.* 2003; Flick *et al.* 2004). As the most elementary setup, the minireplicon system which contains only the expression of viral NP and RdRp proteins along with a minigenome plasmid carrying a reporter gene flanked by the viral UTRs in the viral genomic sense, has been developed for several bunyaviruses, such as Bunyamwera virus (BUNV), Uukuniemi virus (UUKV), Hantaan virus, Crimean-Congo hemorrhagic fever virus (CCHFV), and Rift Valley fever virus (RVFV) (Bergeron *et al.* 2010; Flick *et al.* 2003; Flick and Pettersson, 2001; Gauliard *et al.* 2006; Weber *et al.* 2001). Full reverse genetics systems (*i.e.* rescuing infectious virus entirely from cloned cDNAs) have been also successfully developed for several bunyaviruses, including BUNV, La Crosse virus, UUKV, CCHFV, and RVFV (Bergeron *et al.* 2015; Barr and Wertz 2005; Habjan *et al.* 2008; Rezelj *et al.* 2015), which play crucial roles in understanding virus replication, viral virulence factor and virus-cell interactions (Elliott 2014; Walpita and Flick 2005).

Phylogenetic analysis of the genome sequences divided the SFTSV strains into the Chinese (C) lineage and Japanese (J) lineage. The C lineage contains most strains isolated in China and a few in South Korea and is further classified into 4 genotypes (C1 to C4); while the J lineage contains strains from South Korea, Japan, and a few from China, and is further classified into 3 genotypes (J1 to J3) (Yoshikawa *et al.* 2015). Recent studies suggested that there might be more genotypes of SFTSV (Lv *et al.* 2017; Wu et al. 2017). The genotype diversity presents challenges for the vaccine and antiviral development against SFTS.

Previously, a reverse genetic system was constructed based on strain Hubei 29 pp (HB29pp) belonging to SFTSV genotype C3 and could be efficiently rescued in Vero cells (Brennan *et al.* 2015, 2017). Here, we developed a similar T7 RNA polymerase-based reverse genetics system for a genotype C4 strain. To achieve this, we first re-examined the 5′- and 3′-terminal UTR sequences of the parental strain and developed minireplicon systems based on the L, M, or S UTRs. Then full-length cDNA clones were constructed and infectious viruses were recovered by co-transfecting cells. The rescued virus was characterized by comparison to its parental virus. The system can be applied for future studies to understand the molecular biology of different SFTSV genotypes, as well as for vaccine and antiviral drug development.

Materials and Methods

Cells and Viruses

African green monkey kidney cells (Vero, ATCC CCL-81) were grown in Dulbecco's modified Eagle's medium (DMEM) supplemented with 10% fetal bovine serum (FBS). BSR-T7 cells which stably express T7 RNA polymerase were kindly provided by Dr. Lei-Ke Zhang from Wuhan Institute of Virology, Chinese Academy of Sciences (Li *et al.* 2019), and were cultured in DMEM supplemented with 10% FBS and 1 mg/mL G418. Both cell lines were grown at 37 °C with 5% CO_2.

SFTSV WCH-2011/HN/China/isolate97 (Lam *et al.* 2013) belonging to C4 clade was kindly provided by Prof. Wuchun Cao from State Key Laboratory of Pathogen and Biosecurity, Beijing Institute of Microbiology and Epidemiology, and has been propagated and adapted in Vero cells for dozens of passages in our biosafety level 2 (BSL-2) laboratory before it was stored as viral stocks at –80 °C. To clarify, we named the initial strain as

SFTSV-WCH, and the laboratory-adapted strain as adapted-SFTSV-WCH in this study.

3′ and 5′ RACE Analyses of Adapted-SFTSV-WCH

3′ RACE (rapid amplification of cDNA ends) analysis was used to obtain the 3′ terminal sequences of cRNA using strand-specific primers. In brief, viral RNA was isolated from supernatants of adapted-SFTSV-WCH infected Vero Cells using a PureLink™ Viral RNA/DNA Mini Kit (Invitrogen), and polyadenylated through Poly (A) Tailing Kit (AM1350 Ambion) according to the manufacturer's protocols. Then cDNA was synthesized from the purified RNA using the Oligo (dT) primer (Supplementary Table S1) through Moloney murine leukemia virus (M-MLV) reverse transcriptase (Promega) and used as the templates in the PCR reaction with the 3′ RACE anchor primer and 3′ RACE segment (L, M, or S)- primers (Supplementary Table S1) through KOD Hot Start DNA polymerase (Takara). The amplified products were purified on an agarose gel and the nucleotide sequences were determined.

5′ RACE analysis was performed using 5′ RACE kit (PR6931 BioTeke Corporation). cDNA of L/M/S was respectively synthesized by reverse transcription PCR (RT-PCR) using segment specific RT primers (Supplementary Table S1). The purified cDNA was added with homopolymeric tails in the TdT-tailing reaction, and used as the templates in the PCR reaction with 5′ RACE anchor primer and segment-specific PCR primers (Supplementary Table S1). The amplified products were purified and sequenced.

Plasmids

Plasmids expressing minigenomes were created according to previous description (Brennan *et al.* 2015). Briefly, the internal sequence of L, M, and S segments were obtained from cells infected with SFTSV-WCH by RT-PCR. The NP and RdRp ORFs were cloned into pCAGGS vector between *Kpn*I and *Not*I restriction enzyme digestion sites (Takara), resulting in pCAGGS-NP and pCAGGS-RdRp. The UTR sequences of the three segments were obtained from adapted-SFTSV-WCH infected cells by RACE analysis as described above. The L/M-segments based constructs contained the enhanced green fluorescent protein (eGFP) ORF sequence between a T7 promoter and a hepatitis delta virus ribozyme (HDVR) sequence in negative sense flanked by viral genomic sense L/M-UTR sequences in T7 vector and were called pT7-L-UTR-eGFP and pT7-M-UTR-eGFP, respectively. The T7 vector was kindly provided by Dr. Lei-Ke Zhang from Wuhan Institute of Virology, Chinese Academy of Sciences. In the S-segment-based minigenome, the NSs ORF except the last 11 amino acids was replaced by eGFP protein, and was named pT7-delNSs: eGFP.

Plasmids for the recovery of SFTSV were constructed according to Brennan *et al.* (2015). The full-length cDNAs of L, M, and S were obtained by connecting the UTR sequences to the corresponding inner sequences by overlap PCR using the primers (Supplementary Table S1) with the fusion region of T7 vector. Then the full-length cDNAs were cloned into T7 vector between a T7 promoter and a HDVR sequence by In-Fusion HD restriction-free cloning (Clontech) in viral complementary orientation, and were named pT7-L, pT7-M, and pT7-S, respectively. The cDNAs were positioned precisely at the sites of transcriptional initiation and ribozyme-mediated cleavage, respectively, in order to achieve transcription of RNAs which had no additional nucleotides at either terminus by following autocatalytic cleavage by the HDV ribozyme.

Minigenome Assay

To optimize the conditions for minigenome system, BSR-T7 cells were seeded in 12-well plates to achieve 75% confluence, and then transfected with 0.5 μg pCAGGS-NP and various amounts of pCAGGS-RdRp or 1 μg pCAGGS-RdRp and various amounts of pCAGGS-NP, together with the 0.5 μg T7-M-UTR-eGFP using Lipofectamine 3000, according to the manufacturer's instructions (Invitrogen). At 36 h post-transfection (p.t.), the green fluorescence was observed under fluorescence microscope to assay the effect of the minigenome. On this basis, the L, M, S-based minigenomes were generated with the optimal amount of the ribonucleoproteins by co-transfecting 0.5 μg pCAGGS-NP, 1 μg pCAGGS-RdRp, together with 0.5 μg plasmid of T7-L-UTR-eGFP, or T7-M-UTR-eGFP, or T7-delNSs: eGFP into BSR-T7 cells described as above, while the negative controls were generated by transfecting function minigenome but lacking the expressing plasmid pCAGGS-NP or pCAGGS-RdRP or both two.

Immunofluorescence Assays (IFAs)

To detect viral protein expression in cells, cells were fixed with 4% paraformaldehyde and permeabilized with 0.3% TritonX-100. IFA was performed using 1:500 diluted polyclonal antibodies against SFTSV NP (anti-NP) (Zhang *et al.* 2017) as primary antibody and 1:500 diluted goat anti-rabbit serum conjugated with fluorescein isothiocyanate (FITC) (Abcam, UK) as the secondary antibody. The green fluorescence was visualized using a fluorescence microscope (ECLIPSE TE2000-S; Nikon, Japan).

Virus Rescue

BSR-T7 cells were cultured in twelve-well plates with 75% confluence and transfected with pCAGGS-NP (0.5 μg), pCAGGS-RdRp (0.5 μg), pT7-L (1 μg), pT7-M (1 μg), and pT7-S (1 μg) through Lipofectamine™ 3000 Transfection Reagent (ThermoFisher) at 37 °C. At 4 days p.t., the virus-containing supernatant (passage 0, P0) was transmitted to fresh Vero cells and incubated at 37 °C for 4 days (passage 1, P1), and the passage was continued. 0.5 mL of virus-containing supernatant of per passage was collected for infectivity analysis.

Virus Titration by Immunostaining

Vero cells seeded in 24-well plates with 100% confluence were incubated with ten-fold serial concentration of the viruses diluted in DMEM at 37 °C for 1.5 h, and followed by adding an overlay consisting of DMEM supplemented with 2% FBS and 1% (w/v) Avicel (Millipore). After incubation at 37 °C for 7 days, the overlay was removed, and the cells were fixed with 4% formaldehyde and permeabilized with 0.3% Triton X-100. The fixed cells were probed with a 1:200 dilution of anti-NP followed by 1:1,000 dilution of horseradish peroxidase (HRP)-labeled anti-rabbit IgG (Sigma). Visualization of viral foci was accomplished by using HRP-DAB Substrate (PA110 TIANGEN). Viral titers were calculated as plaque forming unit (PFU) per milliliter (mL).

One-Step Growth Curve Analyses

Vero cells cultured in 6-well plates were infected with viruses at a multiplicity of infection (MOI) of 1 PFU/mL. Fifty microliters of supernatant was harvested from each sample at different time points post infection (p.i.). Virus titers were measured by immunostaining described as above. The experiments were performed in two repeats. All data was analyzed using GraphPad Prism 8.0 software (GraphPad Software Inc.). Student's *t* tests were used to determine differences between two groups and statistical significance was assigned when P values were < 0.05.

Virus Whole-Genome Sequencing

The viral RNA was extracted from the supernatants of infected cell culture using a PureLink™ Viral RNA/DNA Mini Kit. The RNA samples were sent to Novogene for constructing RNA libraries followed by sequencing using BGI MGISEQ-2000. The raw reads were firstly processed by Cutadapt (v.1.18) to get the clean data which were mapped to the GenBank reference sequences of SFTSV (JQ341188.1, JQ341189.1, and JQ341190.1) for comparison and analyzed by Bowtie2.

Western Blotting

To detect viral protein expression, the infected cells were lysed in RIPA lysis buffer (Bryotime) at different time points after infection. Then cellular samples were fractionated by SDS–polyacrylamide gel electrophoresis (SDS-PAGE) and then transferred to polyvinylidene difluoride (PVDF) membranes (Millipore). The blots were probed with SFTSV anti-NP (1:1000) as the primary antibody and horseradish peroxidase goat anti-mouse antibody (1:2000) (Sigma) as the secondary antibody. Visualization of detected proteins was achieved by scanning on a Micro-Chemi imaging system.

Results

Sequencing the UTR Sequences of Adapted-SFTSV-WCH

Initially we failed to generate minireplicon using the UTRs identical to that of SFTSV-WCH published in GenBank (data not shown). As UTR sequences were critical for constructing reverse genetic systems (Brennan *et al.* 2015), we then determined the UTRs sequences of adapted-SFTSV-WCH by 3′ and 5′ RACE. Sequencing of the RACE products revealed several nucleotide changes in all the L/M/S-UTRs of adapted-SFTSV-WCH (Fig. 1, shown in red bases) in comparison to the published SFTSV-WCH sequences (Fig. 1, shown in blue bases in the brackets). For the L segment, we found a change of A to G at position 6 in comparison to the SFTSV-WCH sequence in GenBank (JQ341188.1). For the M segment, two differences were detected at position 6 (A to G) and position 3353 (A to G) comparing to the GenBank sequence (JQ341189.1). For the S segment, we found an additional A at position 10 and one change at position 23 (A to G), compared to the GenBank sequence JQ341190.1 (Fig. 1). The terminal sequences of the 3′- and 5′ UTR for SFTSV were complementary, which permits the formation of a 'panhandle' structure for each segment. The first 9 nt of both 3′ and 5′ termini were relatively conserved among all segments and comprised the conserved complementary region (Fig. 1, sequences in the red box). After these 9 nts, the sequence of the L, M, and S segments were segment specific but still exhibit terminal complementarity up to nucleotide positions 16, 18, and 23, respectively (Fig. 1, sequences in the blue box). In comparison to that of SFTSV-WCH, the adapted-SFTSV-WCH had a unpaired nucleotide at position 6 of the conservation complementary regions of L and M UTRs, and two

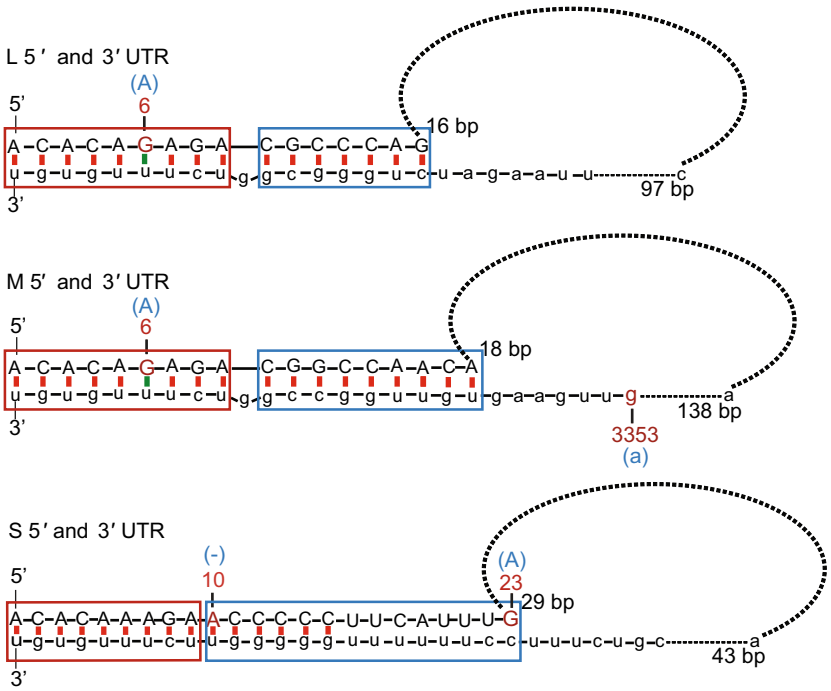

Fig. 1 Schematic of the 3′- and 5′ UTRs of complementary viral RNA. The sequences of 5′ UTR were present in capital letters, and the sequence of 3′ UTR were present in lowercase letters. The corrected nucleotide of the adapted-SFTSV-WCH by RACE analysis was shown in red compared to these published SFTSV-WCH sequences (blue bases in the brackets). Potential to form Watson–Crick base pairs (dash in red) or noncanonical U-G pairings (dash in green) is indicated. The first 9 nt of both 3′ and 5′ termini are relatively conserved between all segments and comprise the conserved complementary region (red boxed sequences), except noncanonical U-G pairings. The variable complementary region of each segment is shown as blue boxed sequences.

nucleotides difference (position 10 and 23) at the variable complementary region of S UTR (Fig. 1).

Development of L/M/S-Based Minigenome Systems for SFTSV

Establishment of the minireplicon system is the first step to ensure that the cloned polymerase is functional and the replication signals are correct before attempting full virus rescue. Therefore, we firstly setup a minireplicon system for SFTSV. The plasmids expressing NP (pCAGGS-NP) and L proteins (pCAGGS-RdRp) were constructed as described in Material and Methods, and the sequences of the ORFs were confirmed to be consistent with those of SFTSV-WCH in the GenBank. The plasmids pT7-L-UTR-eGFP, pT7-M-UTR-eGFP, and pT7-delNSs: eGFP which contained a reporter gene eGFP in the negative sense between the corrected 3′UTR and 5′UTR of cRNA of the L, M and S segments were constructed as described in Materials and Methods (Fig. 2A).

To optimize the conditions for minigenome system, various ratios of the plasmids were used in order to maximize minigenome replication efficiency. M segments-based minigenome plasmid (500 ng pT7-M-UTR-eGFP), and 500 ng pCAGGS-NP with increasing amounts of pCAGGS-RdRp were co-transfected into BSR-T7 cells (Fig. 2B, upper panel). Increasing amounts of RdRp protein in the system generally led to an increase in minigenome activity, and superior effect was achieved with 1,000 ng pCAGGS-RdRp. Then 1,000 ng pCAGGS-RdRp and increasing amounts of pCAGGS-NP were transfected into BSR-T7 cells (Fig. 2B, lower panel), and the optimal effect was obtained with 500 ng pCAGGS-NP and 1,000 ng pCAGGS-RdRp. Therefore, the optimal amounts of the ribonucleoproteins were used for further experiments.

Then the L, M, S-based minigenomes were generated with this optimal amount of the ribonucleoproteins by co-transfection. At 36 h p.t., significant levels of eGFP were expressed from each of the minigenomes, and no green fluorescence was seen in the negative control groups (Fig. 2C). These results revealed that each minigenome RNA contained the correct cis-elements in UTRs, and pCAGGS-NP and pCAGGS-RdRp provided functional trans-factors required for transcription and replication.

Rescue of Infectious Virus from cDNA Clones

In order to recover infectious SFTSV from cloned cDNA, the complete L, M, and S segments were cloned between a

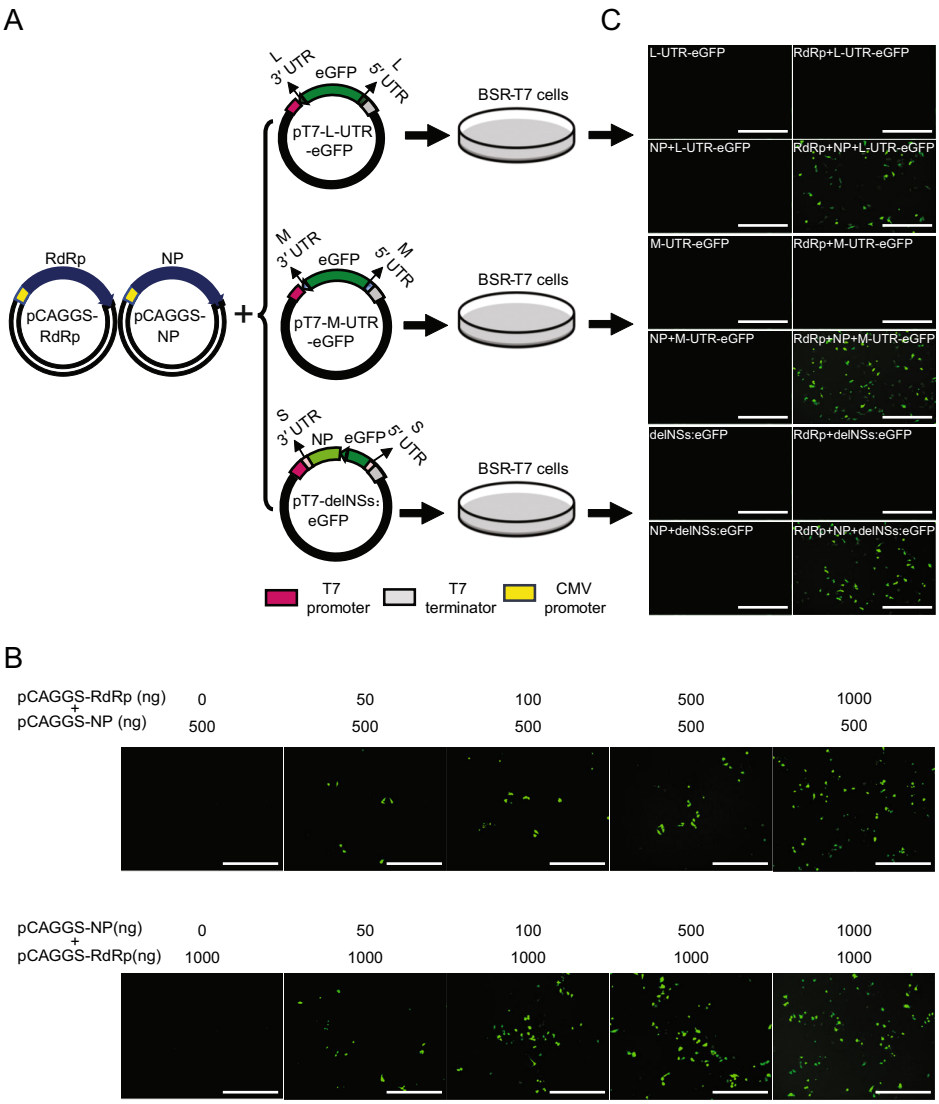

Fig. 2 Creation of the L/M/S-based minigenome constructs. **A** Schematic diagram of the generation of L-, M-, and S-based reporter minigenomes. **B** Effect of increasing amounts of pCAGGS-RdRp (upper panel) or pCAGGS-NP (lower panel) on M-segment minigenome assay. BSR-T7 cells were co-transfected with pT7-M-UTR-eGFP (0.5 μg), and the indicated amounts of pCAGGS-RdRp and pCAGGS-NP. **C** Generation of L/M/S-based minigenomes. BSR-T7 cells were transfected with the minigenome plasmid of pT7-L-UTR-eGFP, pT7-M-UTR-eGFP or pT7-delNSs: eGFP (UTR-eGFP); or co-transfected with the minigenome plasmid and pCAGGS-NP (NP + UTR-eGFP); the minigenome plasmid and pCAGGS-RdRp (RdRP + UTR-eGFP); or the minigenome plasmid with pCAGGS-NP and pCAGGS-RdRp (RdRp + NP + UTR-eGFP). At 36 h post transfection, fluorescence of eGFP was observed. Scale bar: 400 μm.

T7 promoter and a HDVR sequence in viral complementary orientation, resulting in pT7-L, pT7-M, and pT7-S, respectively as described in Material and Methods (Fig. 3A, left). Initial attempts for generating infectious virus by co-transfecting plasmids pT7-L, pT7-M, and pT7-S into BSR-T7 cells, as previously demonstrated successful for other bunyaviruses (Habjan *et al.* 2008), failed to rescue the SFTSV in our hands (data not shown). To improve the rescue efficiency of the system, we supplemented NP and RdRp via co-transfection with expression vectors pCAGGS-NP and pCAGGS-RdRp (Fig. 3A, left). A mixture of pCAGGS-NP, pCAGGS-RdRp, pT7-L, pT7-M, and pT7-S were co-transfected into monolayers of BSR-T7 cells, and the rescued virus at passages 0–3 (P0–P3) were collected as described in Materials and Methods. Infectivity of the P0–P3 viruses were detected in Vero cells by immune fluorescence assay using the anti-NP antibody. As showed in Fig. 3B, initially only a small amount of fluorescence signals were detected in P0 cells, but the amounts of infected cells increased with successive passaging, and the positive rate of viral infected cells had reached approximately 100% in the P3, indicating the infectious recombinant SFTSV virus has been successfully rescued. The rescued virus was named rSFTSV-WCH.

Characterization of the Rescued Virus

To analyze the properties of rSFTSV-WCH, immunostaining assay was conducted using virus-containing supernatant collected from P8. The rescued virus showed foci with similar size and morphology to that of the adapted-SFTSV-WCH (Fig. 4A). Titration analyses revealed that repeated passaging of the rSFTSV-WCH substantially increased virus yield from 4.5×10^3 PFU/mL at P3 to 7.9×10^5 PFU/mL at P8, but the titer of P8 was

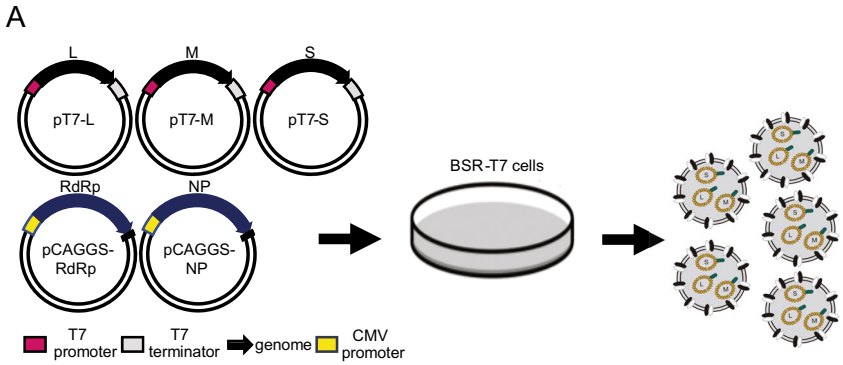

Fig. 3 Rescue of infectious virus from cDNA. **A** General outline of the procedure to generate the rescued virus from cDNA. BSR-T7 cells were transfected pCAGGS-NP, pCAGGS-RdRp, pT7-S, pT7-M, and pT7-L. **B** Detection of the infectivity of the collected supernatants from passage 0 (P0) to P3 by immune fluorescence using the anti-NP antibody. The infectivity of the rescued virus was increasing with passaging from P0–P3, and the positive rate of fluorescent cells had reached 100% in P3. Scale bar: 400 μm.

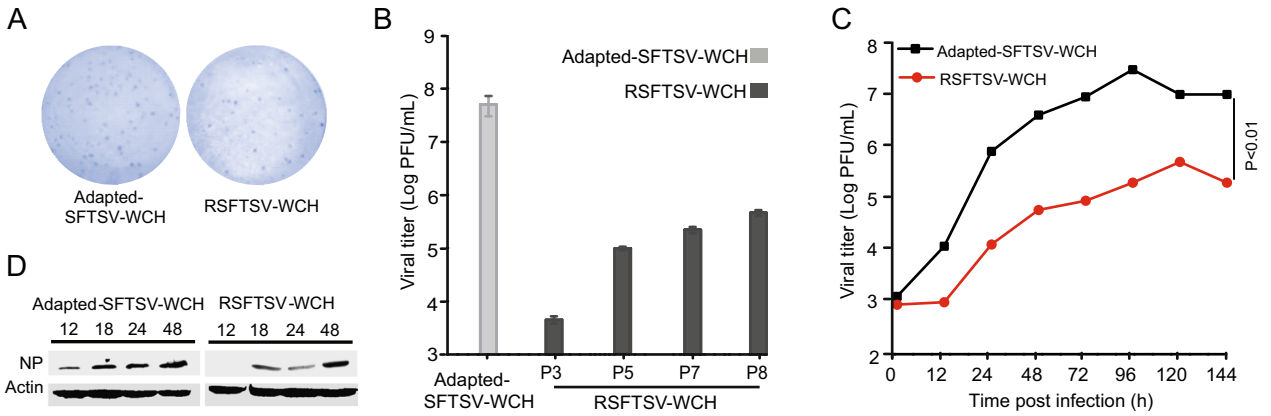

Fig. 4 Characterization of rSFTSV-WCH in comparison to the adapted-SFTSV-WCH. **A** Comparison of immune-stained foci of rSFTSV-WCH and adapted-SFTSV-WCH. **B** The titration of rSFTSV-WCH collected at different passages. The titer of rSFTSV-WCH increased from P3 to P8 but was lower than that of the adapted-SFTSV-WCH. **C** One-step growth curves of rSFTSV-WCH and adapted-SFTSV-WCH conducted in Vero cells at an MOI of 1. *P* values of < 0.01 indicated extremely statistical differences between two groups at any time point. **D** Time-course analysis of nucleoprotein (NP) expression in infected cells. Vero cells were infected with rSFTSV-WCH or adapted-SFTSV-WCH at an MOI of 1, and cellular samples were harvested at the indicated time points for Western blot analysis using anti-NP antibody.

still lower than that of the adapted-SFTSV-WCH which had a titer of 3×10^7 PFU/mL (Fig. 4B).

One-step growth curves of rSFTSV-WCH and adapted-SFTSV-WCH were compared in Vero cells at an MOI of 1. As shown in Fig. 4C, the adapted-SFTSV-WCH grew more efficiently, achieving the maximal titers of 3×10^7 PFU/mL at 96 h p.i., while the rSFTSV-WCH grew to the highest titers of 5×10^5 PFU/mL at 120 h p.i.. And the titers between adapted-SFTSV-WCH and rSFTSV-WCH showed extremely significant difference ($P < 0.01$) at any time points of 12 h, 24 h, 48 h, 72 h, 96 h or 144 h p.i. (Fig. 4C).

Then, the time-course analysis of NP expression was performed by Western blotting. Cells were separately infected with rSFTSV-WCH and adapted-SFTSV-WCH at an MOI of 1, and cellular samples were harvested at 12, 18, 24 and 48 h p.i. As shown in Fig. 4D, NP could be detected at 12 h p.i. in cells infected with adapted-SFTSV-WCH, while it was not detected in rSFTSV-WCH infected cells until 18 h p.i. For both viruses, the intensity of the NP signal keep increasing until 48 h p.i. (Fig. 4D), but the

expression level of NP was lower in the rSFTSV-WCH infected cells than that of the adapted-SFTSV-WCH. These results revealed that the rSFTSV-WCH had lower infectivity than the adapted-SFTSV-WCH.

Comparative Analysis of Genome Sequences of SFTSV-WCH, rSFTSV-WCH, and Adapted-SFTSV-WCH

During the construction of the reverse genetic system, all the inner sequences of the L, M, S segments were confirmed to be consistent to the SFTSV-WCH sequences in the GenBank, while the UTRs have been corrected according to the RACE results of the adapted-SFTSV-WCH. To understand why rSFTSV-WCH had lower infectivity in comparison to that of the adapted-SFTSV-WCH, both viruses were sequenced by RNA-seq and the results were summarized in Table 1. As expected, the UTR sequences of the rSFTSV-WCH were identical to that of adapted-SFTSV-WCH, and the internal L, M and S sequences of rSFTSV-WCH were identical to that of the SFTSV-WCH sequences in GenBank. The adapted-SFTSV-WCH, however, appeared to be a mixture that contained two different nucleotides at nine positions of the internal segments, including 3 positions in L, 5 positions in M, and 1 in S (Table 1). In each of these positions, one of the nucleotides was consistent with the published SFTSV-WCH sequence in GenBank, while the other one appeared to be a new mutation. Apart from the mutation (G) at the 499 nt of M segment which has been appeared in other published SFTSV strains, the rest of the mutations have not been found in any SFTSV strains in the GenBank. Among the three mutations in the L segment, only the one at the 5967 nt position would result in amino acid change (G to E) in the encoding protein, which is not located in the functional motifs of RdRp (Amroun *et al.* 2017). Among the five mutations in the M segment, four (nts 117, 499, 2268 and 3028) resulted in amino acid changes in the encoding proteins. Two of the mutations are within domain I of Gn and one locates in the domain I of Gc (Table 1). Domain I of Gn forms the foundation bed with domain II, while domain I of Gc contributes to pH-induced conformational rearrangemen (Halldorsson *et al.* 2016; Wu *et al.* 2017). For inner sequence of S, there was one new mutation at the position of 556 resulting in amino acid changes (S to T) and this mutation was located between α10 and α11, relatively far from the RNA binding cavity (Jiao *et al.* 2013).

Discussion

There are seven major genotypes of SFTSV (C1-C4 and J1-J3) (Yoshikawa *et al.* 2015) and previously a reverse genetic system was established based on HB29pp belonging to C3 (Brennan *et al.* 2015). The L, M and S segments of genotype C3 strains shared in average about 94%, 93%, and 94% nt identity to that of the genotype C4, respectively, suggesting a relatively high genetic diversity among SFTSV genotypes. Here, we report the establishment of a reverse genetics system based on SFTSV-WCH, a member of C4 clade (Yoshikawa *et al.* 2015). Between HB29pp and SFTSV-WCH strains, there were 250, 147 and 80 nt differences in the L, M, and S segment, respectively. As

Table 1 Comparison of the inner sequences of SFTSV-WCH, rSTFTSV-WCH and adapted-SFTSV-WCH.

Segment	Position[a]	Nucleotide (amino acid)			Other strains[b]	Functional domain[c]
		SFTSV-WCH (GenBank)	rSFTSV-WCH	Adapted- SFTSV-WCH		
L	28	G (E)	G (E)	G/A (E/E)	No	–
	2041	C (V)	C (V)	C-T (V/V)	No	–
	5967	G (G)	G (G)	G/A (G/E)	No	Not in the functional motifs
M	117	C (N)	C (N)	C/A (K/N)	No	Gn (domain I)
	499	A (R)	A (R)	A/G (R/G)	Yes	Gn (domain I)
	2268	C (S)	C (S)	C/A (S/R)	No	Gc (domain I)
	2778	C (S)	C (S)	C/T (S/S)	No	–
	3028	T (Y)	T (Y)	T/C (Y/H)	No	Gc (not in the functional domain)
S	556	G (S)	G (S)	G/C (S/T)	No	Between α10 and α11 of NP

[a]Position in nucleotide sequence.

[b]Whether the mutations appeared in other reported SFTSV strains in GenBank.

[c]Only the mutations which cause amino acid changes were indicated and whether they located in the functional domain of the respective protein or not; –indicated mutations did not cause amino acid changes.

mentioned earlier, due to the failure of establishing the minireplicon by using published UTR sequences of SFTSV-WCH, we conducted 5′ and 3′ RACE of the cRNA of the adapted-SFTSV-WCH to confirm the correctness of UTR sequences. Results revealed several nucleotide changes in all the UTRs of the L/M/S-segments in comparison to the published sequences in GenBank (Fig. 1). The confirmed 5′ UTR sequences were completely consistent with the RACE-corrected UTRs of HB29pp (Brennan *et al.* 2015) but the 3′UTR sequences still have some differences. Then based on the corrected sequences, the minireplicon system for SFTSV-WCH was successfully established (Fig. 2), indicating the UTRs, RdRp- and NP-expressing clones were functional.

For bunyaviruses, the L, M, and S segments exhibit terminal nucleotide complementarity between their 3′ and 5′ UTRs, and the complementarity is critical for RNA synthesis (Barr and Wertz 2004). Like BUNV, the terminal nucleotides of adapted-SFTSV-WCH can be divided into the conserved and variable complementary regions (Fig. 1). After re-examination, we found there was a non-canonical U-G pairings at position 6 in both the L and M UTRs. In BUNV, a non-canonical U-G pairing at conserved complementary regions is strongly preferred for transcription activity in the genomic promoter than the antigenomic promoter (Barr and Wertz 2005). Our results suggested the mutated sequences in the UTRs of adapted-SFTSV-WCH are likely critical for constructing the reverse genetics of the virus. The exact roles of these mutations for viral replication and transcription can be studied in the future.

With the corrected UTR sequences, the infectious rSFTSV-WCH was successfully rescued from the cDNA clones (Fig. 3). The immunostaining foci of the rSFTSV-WCH had the similar size and morphology to that of the adapted-SFTSV-WCH (Fig. 4A). However, after continuous passaging, the infectious virus production of rSFTSV-WCH was still significantly lower than that of the adapted-SFTSV-WCH (Fig. 4B–D). As the adapted-SFTSV-WCH had been cultured for some passages in the laboratory and might obtain mutations prone to the increased infectivity, we therefore conducted whole-genome sequencing of the adapted-SFTSV-WCH and rSFTSV-WCH. The sequencing results revealed that the inner sequences of the rSFTSV-WCH were identical to the original SFTSV-WCH sequence in the GenBank. In contrast, there were 9 positions each of which contained two different nucleobases at the inner sequences of adapted-SFTSV-WCH (Table 1). At each of these positions, one of the nucleotide was in accordance with the GenBank published sequence, while another was new suggesting emerging of mutations during the viral adaption for cell-culture. It is likely some of these mutations resulted in increased infectivity of adapted-SFTSV-WCH. The results also indicated that the adapted-SFTSV-WCH is a mixture of different strains. We are currently purifying the adapted-SFTSV-WCH in order to get different clones and will further confirm which sites are critical for viral infectivity by using the reverse genetic system developed in this study. The infectivity of the rSFTSV-WCH will also be tested in animal models to see if the virus shows any pathological changes, and whether it can be further studied for developing attenuated vaccine.

In conclusion, this study reported the construction and rescue of a recombinant SFTSV from the SFTSV-WCH belonging to C4 clade. The development of the SFTSV reverse genetics system will allow comparative studies of genetic determinants of virulence, critical functions of viral proteins, and designing of live attenuated vaccines. Our future work would focus on the detection of the key positions related to virus infectivity and optimize the efficiency of this system.

Acknowledgements We thank Prof. Wuchun Cao from State Key Laboratory of Pathogen and Biosecurity, Beijing Institute of Microbiology and Epidemiology for providing SFTSV WCH-2011/HN/China/isolate 97; Dr. Leike Zhang from Wuhan Institute of Virology, Chinese Academy of Sciences, for generously providing the BSR-T7 cells. We thank for the assistance from the core faculty of Wuhan Institute of Virology for their critical support; This work was supported by grants from the National Natural Science Foundation of China (No. 31900146; Open Research Fund Program of the State Key Laboratory of Virology of China (No. 2020IOV003); Team project of Health Commission of Hubei Province (WJ2019C003).

Author contributions MW, ZH and JL designed the experiments. MYX and BW conducted the experiments. MYX, MW, ZH and JL wrote the paper. DF and HW edited and commented on the manuscript.

Compliance with Ethical Standards

Conflict of interest The authors declare that they have no conflict of interest.

Animal and Human Rights Statement This article does not contain any studies with human and animal subjects performed by any of the authors.

References

Amroun A, Priet S, de Lamballerie X, Querat G (2017) Bunyaviridae RdRps: structure, motifs, and RNA synthesis machinery. Crit Rev Microbiol 43:753–778

Barr JN, Wertz GW (2004) Bunyamwera bunyavirus RNA synthesis requires cooperation of 3′- and 5′-terminal sequences. J Virol 78:1129–1138

Barr JN, Wertz GW (2005) Role of the conserved nucleotide mismatch within 3′- and 5′-terminal regions of Bunyamwera virus in signaling transcription. J Virol 79:3586–3594

Bergeron E, Albarino CG, Khristova ML, Nichol ST (2010) Crimean-Congo hemorrhagic fever virus-encoded ovarian tumor protease

activity is dispensable for virus RNA polymerase function. J Virol 84:216–226

Bergeron E, Zivcec M, Chakrabarti AK, Nichol ST, Albarino CG, Spiropoulou CF (2015) Recovery of recombinant Crimean Congo hemorrhagic fever virus reveals a function for non-structural glycoproteins cleavage by Furin. Plos Pathog 11:e1004879

Brennan B, Li P, Zhang S, Li A, Liang M, Li D, Elliott RM (2015) Reverse genetics system for severe fever with thrombocytopenia syndrome virus. J Virol 89:3026–3037

Brennan B, Rezelj VV, Elliott RM (2017) Mapping of transcription termination within the S segment of SFTS phlebovirus facilitated generation of NSs deletant viruses. J Virol 91:e717–e743

Cyranoski D (2018) East Asia braces for surge in deadly tick-borne virus. Nature 556:282–283

Elliott RM (2014) Orthobunyaviruses: recent genetic and structural insights. Nat Rev Microbiol 12:673–685

Flick R, Pettersson RF (2001) Reverse genetics system for Uukuniemi virus (Bunyaviridae): RNA polymerase I-catalyzed expression of chimeric viral RNAs. J Virol 75:1643–1655

Flick K, Hooper JW, Schmaljohn CS, Pettersson RF, Feldmann H, Flick R (2003) Rescue of Hantaan virus minigenomes. Virology 306:219–224

Flick K, Katz A, Overby A, Feldmann H, Pettersson RF, Flick R (2004) Functional analysis of the noncoding regions of the Uukuniemi virus (Bunyaviridae) RNA segments. J Virol 78:11726–11738

Gauliard N, Billecocq A, Flick R, Bouloy M (2006) Rift Valley fever virus noncoding regions of L, M and S segments regulate RNA synthesis. Virology 351:170–179

Guardado-Calvo P, Rey FA (2017) The envelope proteins of the Bunyavirales. Adv Virus Res 98:83–118

Habjan M, Penski N, Spiegel M, Weber F (2008) T7 RNA polymerase-dependent and -independent systems for cDNA-based rescue of Rift Valley fever virus. J Gen Virol 89:2157–2166

Halldorsson S, Behrens AJ, Harlos K, Huiskonen JT, Elliott RM, Crispin M, Brennan B, Bowden TA (2016) Structure of a phleboviral envelope glycoprotein reveals a consolidated model of membrane fusion. Proc Natl Acad Sci USA 113:7154–7159

Jiao L, Ouyang S, Liang M, Niu F, Shaw N, Wu W, Ding W, Jin C, Peng Y, Zhu Y, Zhang F, Wang T, Li C, Zuo X, Luan CH, Li D, Liu ZJ (2013) Structure of severe fever with thrombocytopenia syndrome virus nucleocapsid protein in complex with suramin reveals therapeutic potential. J Virol 87:6829–6839

Lam TT, Liu W, Bowden TA, Cui N, Zhuang L, Liu K, Zhang YY, Cao WC, Pybus OG (2013) Evolutionary and molecular analysis of the emergent severe fever with thrombocytopenia syndrome virus. Epidemics-Neth 5:1–10

Li H, Zhang LK, Li SF, Zhang SF, Wan WW, Zhang YL, Xin QL, Dai K, Hu YY, Wang ZB, Zhu XT, Fang YJ, Cui N, Zhang PH, Yuan C, Lu QB, Bai JY, Deng F, Xiao GF, Liu W, Peng K (2019) Calcium channel blockers reduce severe fever with thrombocytopenia syndrome virus (SFTSV) related fatality. Cell Res 29:739–753

Liu Y, Li Q, Hu W, Wu J, Wang Y, Mei L, Walker DH, Ren J, Wang Y, Yu XJ (2012) Person-to-person transmission of severe fever with thrombocytopenia syndrome virus. Vector Borne Zoonotic Dis 12:156–160

Liu J, Xu M, Tang B, Hu L, Deng F, Wang H, Pang DW, Hu Z, Wang M, Zhou Y (2019) Single-particle tracking reveals the sequential entry process of the Bunyavirus severe fever with thrombocytopenia syndrome virus. Small 15:e1803788

Lv Q, Zhang H, Tian L, Zhang R, Zhang Z, Li J, Tong Y, Fan H, Carr MJ, Shi W (2017) Novel sub-lineages, recombinants and reassortants of severe fever with thrombocytopenia syndrome virus. Ticks Tick-borne Dis 8:385–390

Maes P, Adkins S, Alkhovsky SV, Avsic-Zupanc T, Ballinger MJ, Bente DA, Beer M, Bergeron E, Blair CD, Briese T et al (2019) Taxonomy of the order Bunyavirales: second update 2018. Arch Virol 164:927–941

Mcmullan LK, Folk SM, Kelly AJ, Macneil A, Goldsmith CS, Metcalfe MG, Batten BC, Albarino CG, Zaki SR, Rollin PE, Nicholson WL, Nichol ST (2012) A new phlebovirus associated with severe febrile illness in Missouri. N Engl J Med 367:834–841

Park SW, Ryou J, Choi WY, Han MG, Lee WJ (2016) Epidemiological and clinical features of severe fever with thrombocytopenia syndrome during an outbreak in South Korea, 2013–2015. Am J Trop Med Hyg 95:1358–1361

Rezelj VV, Overby AK, Elliott RM (2015) Generation of mutant Uukuniemi viruses lacking the nonstructural protein NSs by reverse genetics indicates that NSs is a weak interferon antagonist. J Virol 89:4849–4856

Takahashi T, Maeda K, Suzuki T, Ishido A, Shigeoka T, Tominaga T, Kamei T, Honda M, Ninomiya D, Sakai T et al (2014) The first identification and retrospective study of Severe Fever with Thrombocytopenia Syndrome in Japan. J Infect Dis 209:816–827

Tran XC, Yun Y, Van An L, Kim SH, Thao NTP, Man PKC, Yoo JR, Heo ST, Cho NH, Lee KH (2019) Endemic Severe Fever with Thrombocytopenia Syndrome, Vietnam. Emerg Infect Dis 25:1029–1031

Walpita P, Flick R (2005) Reverse genetics of negative-stranded RNA viruses: a global perspective. Fems Microbiol Lett 244:9–18

Walter CT, Barr JN (2011) Recent advances in the molecular and cellular biology of bunyaviruses. J Gen Virol 92:2467–2484

Wang Y, Deng B, Zhang J, Cui W, Yao W, Liu P (2014) Person-to-person asymptomatic infection of severe fever with thrombocytopenia syndrome virus through blood contact. Intern Med 53:903–906

Weber F, Dunn EF, Bridgen A, Elliott RM (2001) The Bunyamwera virus nonstructural protein NSs inhibits viral RNA synthesis in a minireplicon system. Virology 281:67–74

Wu Y, Zhu Y, Gao F, Jiao Y, Oladejo BO, Chai Y, Bi Y, Lu S, Dong M, Zhang C, Huang G, Wong G, Li N, Zhang Y, Li Y, Feng WH, Shi Y, Liang M, Zhang R, Qi J, Gao GF (2017) Structures of phlebovirus glycoprotein Gn and identification of a neutralizing antibody epitope. Proc Natl Acad Sci USA 114:E7564–E7573

Yoshikawa T, Shimojima M, Fukushi S, Tani H, Fukuma A, Taniguchi S, Singh H, Suda Y, Shirabe K, Toda S, Shimazu Y, Nomachi T, Gokuden M, Morimitsu T, Ando K, Yoshikawa A, Kan M, Uramoto M, Osako H, Kida K, Takimoto H, Kitamoto H, Terasoma F, Honda A, Maeda K, Takahashi T, Yamagishi T, Oishi K, Morikawa S, Saijo M (2015) Phylogenetic and geographic relationships of severe fever with thrombocytopenia syndrome virus in China, South Korea, and Japan. J Infect Dis 212:889–898

Yu XJ, Liang MF, Zhang SY, Liu Y, Li JD, Sun YL, Zhang L, Zhang QF, Popov VL, Li C, Qu J, Li Q, Zhang YP, Hai R, Wu W, Wang Q, Zhan FX, Wang XJ, Kan B, Wang SW, Wan KL, Jing HQ, Lu JX, Yin WW, Zhou H, Guan XH, Liu JF, Bi ZQ, Liu GH, Ren J, Wang H, Zhao Z, Song JD, He JR, Wan T, Zhang JS, Fu XP, Sun LN, Dong XP, Feng ZJ, Yang WZ, Hong T, Zhang Y, Walker DH, Wang Y, Li DX (2011) Fever with thrombocytopenia associated with a novel bunyavirus in China. N Engl J Med 364:1523–1532

Zhang Y, Shen S, Shi J, Su Z, Li M, Zhang W, Li M, Hu Z, Peng C, Zheng X, Deng F (2017) Isolation, characterization, and phylogenic analysis of three new severe fever with thrombocytopenia syndrome bunyavirus strains derived from Hubei Province, China. Virol Sin 32:89–96

Zhao L, Zhai S, Wen H, Cui F, Chi Y, Wang L, Xue F, Wang Q, Wang Z, Zhang S, Song Y, Du J, Yu XJ (2012) Severe fever with thrombocytopenia syndrome virus, Shandong Province, China. Emerg Infect Dis 18:963–965